Numerical Study of Double Diffusive Convection in presence of Radiating Gas in a Square Cavity

F. Moufekkir[1]**, M.A. Moussaoui**[1]**, A. Mezrhab**[1,2]**, H. Naji**[3,4] **and M. Bouzidi**[5]

Abstract: The problem related to coupled double diffusive convection in a square enclosure filled with a gray gas in the presence of volumetric radiation is examined numerically. The horizontal walls are assumed to be insulated and impermeable. Different temperatures and species concentrations are imposed at vertical walls. In particular, we propose a 2-D numerical approach based on a hybrid scheme combining a multiple-relaxation-time lattice Boltzmann model (MRT-LBM) and a standard finite difference method (FDM). The radiative term in the energy equation is treated using the discrete ordinates method (DOM) with a S8 quadrature. The influence of various parameters (such as the Rayleigh number, the buoyancy number, the optical thickness and Lewis number) on fluid flow, heat and mass transfer is evaluated. Results show that for the case of cooperating flows, the isotherms and isoconcentrations are inclined in the core cavity and the flow is relatively stable whereas multicellular recirculations appear in the opposing-flows case. Generally when the mass effect is dominant, the flow is slowed and the influence of radiation is considerable on the thermal field and negligible on the dynamic and concentration fields. However, when thermal effects are dominant, the volumetric radiation accelerates the flow and significantly alters the structure of velocity, concentration and temperature fields.

Keywords: Numerical analysis, heat transfer, convection, volumetric radiation, Lattice Boltzmann Method, Discrete ordinate Method.

---

[1] Laboratoire de Mécanique & Energétique, Faculté des sciences, Département de physique, 60000 Oujda, Maroc.

[2] Correspondence author: amezrhab@yahoo.fr.

[3] Laboratoire Génie Civi & géo-Environnement (LGCgE- EA 4515), UArtois/FSA Béthune, F-62400 Béthune, France.

[4] Université Lille Nord de France, F-59000 Lille/Université d'Artois/FSA, F-62400 Béthune, France.

[5] Institut Pascal UBP/CNRS/IFMA, IUT d'Allier, B.P. 2235, Avenue Aristide Briand, 03101 Montluçon cedex.

Nomenclature

C	molecular concentration, m^{-3}
g	gravitational acceleration, $m.s^{-2}$
i_0	black body radiation intensity, $Wm^{-2}sr^{-1}$
I	dimensionless radiation intensity, $= i/4\sigma T_0^4$
k	thermal conductivity, $Wm^{-1}K^{-1}$
L	enclosure width, m
Le	Lewis number, $= \alpha/D$
Nu_T	average total Nusselt number at the side walls
Pl	Planck number, $= (k/L)/(4\sigma T_0^4)$
Pr	Prandtl number, $= \nu/\alpha$
Q_R	dimensionless radiative heat flux, $= q_R/4\sigma T_0^4$
Ra	Rayleigh number, $= g\beta(T_h - T_c)L^3/\nu\alpha$
S	dimensionless concentration, $= [(C - C_0)/\Delta C]$
T_h, T_c	hot and cold wall temperatures, K
T_0	average temperature, $=(T_h + T_c)/2$, K
U, V	dimensionless velocity components, $(U = uL/\alpha, V = vL/\alpha)$
X, Y	dimensionless coordinates, (X=x/L,Y=y/L)

Greek symbols

α	thermal diffusivity, $m^2.s^{-1}$
$\beta_{T(C)}$	thermal (mass) expansion coefficient, K^{-1} (m^3)
ε	emissivity of radiative surface
ϕ	inclination angle, K
μ, ξ	direction cosines
ν	kinematic viscosity, $m^2.s^{-1}$
σ	Stefan-Boltzmann constant, $W.K^{-4}.m^{-2}$
Ω	collision operator
τ_0	optical thickness
θ	dimensionless temperature, $= (T - T_0)/(T_h - T_c)$
Θ_0	reference temperature ratio, $= T/(T_h - T_c)$
Ψ	dimensionless stream function
ω	scattering albedo

1 Introduction

The double-diffusive natural convection continues to be a very attractive subject in research in reason to its importance in natural and industrial applications such as oceanography, astrophysics, geophysics, petrology, food processing, chemical processes, crystal growth process and solidification in material processing, etc. This phenomenon occurs when the flow is generated by buoyancy due to simultaneous temperature and concentration gradients. Reviews on this subject can be found in the publications of [Hu and El-Wakil (1974)], [Trevisan and Bejan (1987)], [Viskanta; Bergman and Incopera (1985)], [Mohamad; Bennacer and El-Ganaoui (2010)], [Choukairy; Bennacer; Beji; El Ganaoui and Jaballah (2006)], [Gobin; Goyeau and Neculae (2005)] and [Ghorayeb; Khallouf and Mojtabi (1999)].

Recently, most attention was focused on the coupling of natural convection (single or double diffusive) and radiation owning to its prominent engineering applications. As consequence, several studies have been carried out on the interaction of radiation and natural convection in a rectangular cavity differentially heated containing a gray fluid participating in emission and absorption ([Balaji and Vankateshan (1994)], [Lauriat (1982)], [Tan and Howell (1991)], [Kassemi and Naraghi (1993)] and [Yucel; Acharya and Williams (1989)]). From these works, the investigation of coupled natural convection and radiation can be classified into two categories. In the first categories, only the surface radiation (the fluid is assumed to be transparent) is taking into account. In the second category, the radiative participation of fluid (fluid semi-transparent) is considered. In the light of these studies, one can conclude that the surface radiation changes significantly the temperature distribution at low Rayleigh number and contributes at the increase of the total heat flux by more than the half. The results showed also that volumetric radiation intensifies the velocity fields for high Rayleigh numbers and standardizes the temperature field. In addition the discrete ordinate method was found more accurate than the P1 method to evaluate the radiative information [Yucel; Acharya and Williams (1989)].

Concerning coupled double diffusive convection and volumetric radiation, generally in the related literature, the active fluid was always considered as a medium with a uniform absorption.

[Ganesan and Loganathan (2002)] have considered this type of coupling for a two-dimensional flow around a semi-infinite vertical cylinder placed in a gray radiative participating fluid using the Rosseland approximation to compute the radiative flux. A little later, [Ramachandra Prasad; Bhaskar Reddy and Muthucumaraswamy (2007)] have considered the same problem for an infinite vertical plate. [Borjini; Ben Aissia; Halouani and Zeghmati (2006)] studied the effects of radiative properties of a semitransparent medium on double diffusive natural convection in the

presence of an external magnetic field in a rectangular cavity using the finite volume method. The authors concluded that the radiative effects are greater when the thermal forces are dominant or comparable to mass forces. Indeed these effects increase the velocity fields in the cavity core, destroy the symmetry of the dynamic, thermal and concentration fields and reduce the total heat flux.

The present work is focused on double diffusive convection in presence of volumetric radiation where the fluid is a binary mixture which absorbs and emits radiation depending to its local concentration (or temperature). This assumption is only addressed by [Rafieivand (1999)] and [Mezrhab; Lemonnier; Meftah and Benbrik (2008)], [Moufekkir; Moussaoui; Mezrhab; Lemonnier and Naji (2012)]. The hybrid scheme based on MRT-LBM and FDM coupled to DOM has not been previously used at the author's best knowledge.

The LBM is considered actually as an efficient CFD tool owning to the advantages that can provide as the simplicity in calculation, the adaptation to complex geometries and boundary conditions, stability, accuracy and gain in computing time.

The use of the numerical combination between HTLBM and DOM is recommended since the hybrid scheme of the LBM and the finite differences method has proven its capability to solve various complicated problems [Mezrhab; Moussaoui and Naji (2008)], [Moussaoui; Jami; Mezrhab and Naji (2010)], [Lallemand and Luo (2000)], [Lallemand and Luo (2003)], [Semma; El Ganaoui and Mohamad (2008)] and also because the DOM was found more accurate and compatible when it's coupled with others CFD solvers [Yucel; Acharya and Williams (1989)].

The aim of this work is to study numerically the double diffusive natural convection in square cavity asymmetrically heated filled with gray gas, the numerical approach adopted uses a hybrid scheme with lattice Boltzmann method (LBM-MRT) for fluid velocity variables, the finite difference method (FDM) for solving differential equations governing the transfer of energy and mass and the radiative source term in energy equation is evaluated using the discrete ordinate method (DOM). Some physical parameters are studied numerically to highlight their effect on the flow, temperature and concentration fields such as the ratio of buoyancy forces and thermal mass, the opacity of the fluid, the Rayleigh number and the Lewis number.

2   Model and Formulation

As represented in Fig. 1, the physical model consists of an asymmetrically heated square cavity filled with a binary gas which is considered as gray, Newtonian, incompressible and participating in emission and absorption. The vertical walls are maintained at temperatures (T_h, T_c) and concentrations (C_c, C_h), while the horizontal walls are perfectly insulated and impermeable to mass transfer.

Natural convection of double diffusion occurs when the flow is generated by buoyancy due to simultaneous temperature and concentration gradients. Cooperating or opposing flows can take place depending to the boundary conditions configuration on the temperatures and the concentrations at active walls. The basic assumptions considered presume that the convective flow is two-dimensional and laminar, the viscous heat dissipation is neglected in the energy equation and all physical properties are constants except for the density, which is assumed to vary in the Boussinesq sense. Furthermore, the density of the mixture is assumed to be lower than that of the impurity and the pollutant is assumed to participate in radiation depending of the impurity absorption coefficient. So, the fluid density is done by [Trevisan and Bejan (1987)]:

$$\rho = \rho_0[1 - \beta_T(T - T_0) - \beta_C(C - C_0)] \tag{1}$$

where β_T and β_C are respectively defined by:

$$\beta_T = -\frac{1}{\rho_0}\left(\frac{\partial \rho}{\partial T}\right)_C \tag{2}$$

and

$$\beta_S = -\frac{1}{\rho_0}\left(\frac{\partial \rho}{\partial C}\right)_T$$
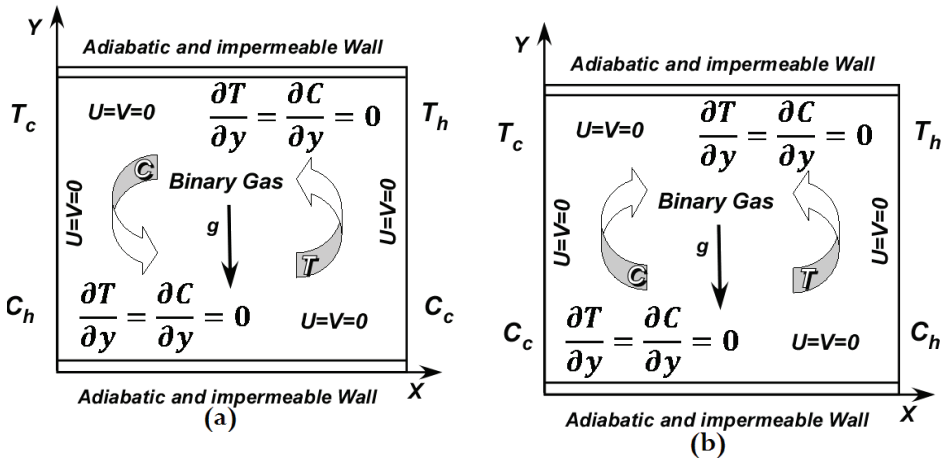

Figure 1: Physical model: (a) aiding flow case, (b) opposing flow case.

2.1   Lattice Boltzmann equation

Actually, the Lattice Boltzmann models (LBM) is considered as an alternative CFD tool, on the ground of its remarkable ability to simulate fluid flows. The evolution of this model consists in two steps that take place during each time step (advection and collision).

In this study, we use the multiple relaxation time Boltzmann equation (MRT-LBE) model, this model was developed by [D'Humières (1992)] to enhance the stability of the LBE in the low viscosity regime. Consider a two-dimensional model of the LBM method to nine discrete velocities called D2Q9 model on a square grid with $\delta x = \delta y = 1$. The fluid particles moves from one grid node to neighbouring node with discrete velocities are given by:

$$
e_i = \begin{cases} (0,0), & i = 0 \\ (\cos\left[(i-1)\pi/2\right], \sin([(i-1)\pi/2]))\,c, & 1 \le i \le 4 \\ \sqrt{2}\,(\cos\left[(2i-9)\pi/4\right], \sin\left([(2i-9)\pi/4]\right))\,c, & 5 \le i \le 8 \end{cases} \tag{3}
$$

where $c = \delta x / \delta t$, with $\delta t = 1$, the time step.

The equation of time evolution of the fluid state is:

$$
f_i(x + e_i, t + 1) - f_i(x,t) = \Omega f_i(x,t) \quad i = 0, \dots, 8 \tag{4}
$$

where f_i is the distribution function of a particle, Ω is the collision operator and x is the node where the particle is localised at time t. The linearization of this operator around the distribution function in local equilibrium f_i^{eq} brings a significant simplification of the method LBM.

With BGK approximation [Bhatnagar; Gross and Krook (1954)], Eq. (4) can be written as:

$$
f_i(x + e_i, t + 1) - f_i(x,t) = \frac{1}{\chi}\left(f_i(x,t) - f_i^{eq}(x,t)\right) \tag{5}
$$

where χ is the relaxation time defined by: $\chi = 3\nu + 0.5$.

In each domain node, we compute a set of nine times, $M(x,t) = \{m_1\,(x,t), m_2\,(x,t),\dots, m_9\,(x,t)\}$, associated with the nine distribution functions, $F(x, t) = \{f_1\,(x, t), f_2\,(x, t),\dots, f_9\,(x,t)\}$, which are related by the linear transformation [Lallemand and Luo (2000)]:

$$
M = P.F \quad F = P^{-1}.M \tag{6}
$$

where P is the matrix of passage from F to M and P^{-1} is the inverse matrix.

During the collision step, which is local operation in space, three moments are conserved (the density and the components of momentum), the six remaining moments, non conserved, are calculated from a simple linear equation in reason to be relaxed to the equilibrium values which depend on conserved quantities:

$$m_k^c = m_k + s_k \left(m_k^{eq} - m_k \right), \quad k = 3, ..., 8 \tag{7}$$

where $s_k = \Delta t / \chi$ is the relaxation rate, m_k^c the moment after collision and m_k^{eq} is the moment at equilibrium.

After the collision step, the new distribution functions f^c are calculated from the new times:

$$f^c = P^{-1}.m^c \tag{8}$$

The density and velocity are given by:

$$\rho(x,t) = \sum_i f_i(x,t), \quad u(x,y) = \sum_i f_i(x,t) e_i / \rho(x,t) \tag{9}$$

2.2 Energy and mass equations

According to the stated assumptions, the energy and species equations are derived as follows:

Energy:

$$U \frac{\partial \theta}{\partial X} + V \frac{\partial \theta}{\partial Y} = \left(\frac{\partial^2 \theta}{\partial X^2} + \frac{\partial^2 \theta}{\partial Y^2} \right) - \frac{\Theta_0}{Pl} \nabla \cdot Q_R \tag{10}$$

Concentration:

$$U \frac{\partial S}{\partial X} + V \frac{\partial S}{\partial Y} = \frac{1}{Le} \left(\frac{\partial^2 S}{\partial X^2} + \frac{\partial^2 S}{\partial Y^2} \right) \tag{11}$$

As shown by [Yucel; Acharya and Williams (1989)], the radiative source term, in the energy equation is evaluated by solving the radiative transport equation (RTE). In fact for each of the finite number of directions $(\overrightarrow{\Omega_m})$, $m = 1, M$, the luminance field $I(X,Y,\overrightarrow{\Omega_m}) = I_m(X,Y)$ is calculated on the entire domain by solving the following equation:

$$\mu \frac{\partial I_m}{\partial X} + \xi \frac{\partial I_m}{\partial Y} + \tau I_m = \frac{\tau}{4\pi} \left[(1 - \omega) \left(1 + \frac{\theta}{\Theta_0} \right)^4 + \omega \int_{4\pi} I d\Omega \right] \tag{12}$$

where τ is the opacity of the medium. Then the integrals of the incident radiation and the radiative flux vector by quadrature are done by:

$$G = \int_{4\pi} I d\Omega = \sum_{m=1}^{M} W_m I_m$$

and

$$\overrightarrow{Q_R} = \int_{4\pi} \overrightarrow{\Omega} I d\Omega = \sum_{m=1}^{M} W_m I_m \Omega_m \tag{13}$$

where the coefficient W_m is the weight of the quadrature, μ, ξ are direction cosines and I_0 is the black body luminance. Reviews on this subject can be found in the publications of [Chandrasekhar (1950)], [Truelove (1988)] and [Fiveland (1984)].

Owing to the boundary conditions used for concentration, $N \geq 0$ stands for the cooperating flow and $N \leq 0$ for the opposite flow. In the present, the boundary conditions are expressed as:

- At the left cold wall: $U = V = 0$, θ_c = -0.5, S_c=0.5 for aiding case (-0.5 for an opposite flow).

- At the right hot wall: $U = V = 0$, $\theta_h = 0.5$, S_h= - 0.5 for aiding case (0.5 for an opposite flow).

- At the adiabatic walls: $U = V = 0$, $\frac{\partial S}{\partial Y} = 0$,

$$\frac{\partial \theta}{\partial Y} - \frac{\Theta_0}{Pl} \varepsilon_W \left[\frac{1}{4} \left(1 + \frac{\theta}{\Theta_0} \right)^4 - \int_{\overrightarrow{n}.\overrightarrow{\Omega'}<0} \left| \overrightarrow{n}.\overrightarrow{\Omega'} \right| I \left(X, Y, \overrightarrow{\Omega'} \right) d\Omega' \right] = 0.$$

2.3 *Heat and mass transfer*

The heat transfer through the cavity is characterized by the Nusselt number, which, in our problem, involves a radiative contribution. The averaged Nusselt number along the Y-axis is expressed by:

$$Nu_T (X_W) = \frac{1}{A}$$

$$\int_0^A \left\{ -\left[\frac{\partial \theta}{\partial X} \right]_{X_W,Y} + \frac{\Theta_0}{Pl} \varepsilon_W \left[\frac{1}{4} \left(1 + \frac{\theta}{\Theta_0} \right)^4 - \int_{\overrightarrow{n}.\overrightarrow{\Omega'}<0} \left| \overrightarrow{n}.\overrightarrow{\Omega'} \right| I \left(X, Y, \overrightarrow{\Omega'} \right) d\Omega' \right] \right\} dY$$

$$\tag{14}$$

In other side, the mass transfer in the enclosure is done by the Sherwood number. The averaged Sherwood number along the side walls is given by:

$$Sh(X_w) = -\frac{1}{A} \int_0^A \left. \frac{\partial S}{\partial X} \right|_{X_w Y} dY \tag{15}$$

2.4 Validation

In this investigation, the computer code was checked for accuracy against the earlier published numerical results reported in the literature related to heat and mass transfer in asymmetrically heated square enclosures.

The numerical code is validated for double diffusive natural convection in the presence of gray gas (Tab. 1) at Ra=5.10^6 and N=4. Our results are compared with those of [Mezrhab; Lemonnier; Meftah and Benbrik (2008)], [Rafieivand (1999)] and [Meftah (2010)]. As can be seen, the Nu_c and Nu_T are successfully compared to those given by the cited references with a maximal deviation about 1.57% for total Nusselt number.

Table 1: Code validation in coupled double diffusive convection and volumetric radiation for Ra=5.10^6 and N=4. Note that here, the abbreviation CW means current work.

τ	**Nu_C**				**Nu_T**			
	Meftah (2010)	Rafieivand (1999)	Mezrhab (2008)	**CW**	Meftah (2010)	Rafieivand (1999)	Mezrhab (2008)	**CW**
0.1	21.66	21.77	21.59	21.62	56.62	56.9	56.35	56.29
1	21.83	22.06	21.82	21.78	48.55	48.9	48.06	48.14
5	19.86	19.83	19.82	19.77	36.12	36.25	35.81	35.79

To be sure about the accuracy and the reliability of the present code, we compared the structures of streamlines, iso-concentrations and isotherms with those available in the literature. Fig. 2 shows that the results obtained with our code compare very well to those given by, [Rafieivand (1999)], [Mezrhab; Lemonnier; Meftah and Benbrik (2008)] and [Meftah (2010)].

From these findings, the code is deemed fit to evaluate the effect of physical parameters characterizing the problem on the temperature, concentration and flow fields.

3   Results and discussion

In this section, two types of flows, opposing (heat and mass buoyancy forces are opposite) and cooperating (heat and mass buoyancy forces cooperate) are studied for the double diffusive convection in the presence of radiation, in steady regime.
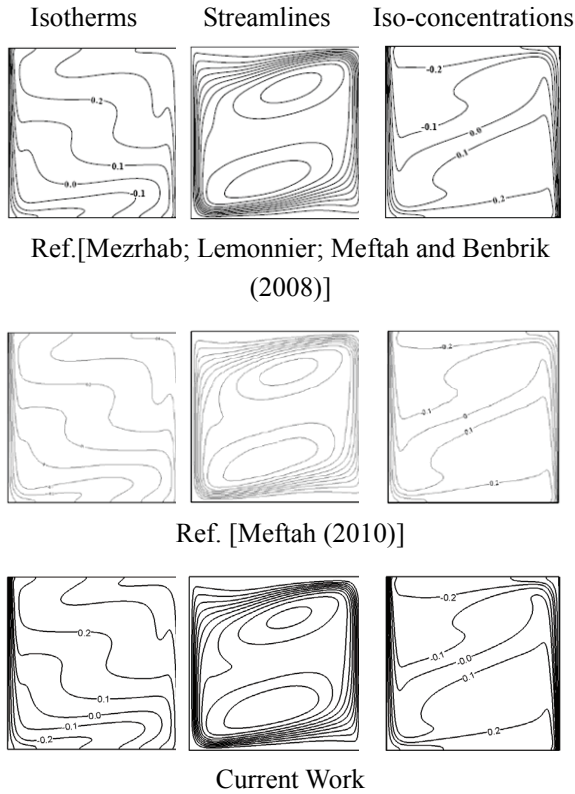
Isotherms   Streamlines   Iso-concentrations

Ref.[Mezrhab; Lemonnier; Meftah and Benbrik
(2008)]

Ref. [Meftah (2010)]

Current Work

Figure 2: Validation code with streamlines, iso-concentrations and isotherms for Ra=5.10^6, N=1

The configuration considered is a square cavity, filled with a binary gas. The left and right vertical walls are kept isothermal at the hot (T$_h$) and cold (T$_c$) temperatures, respectively. For the mixture with pollutant, zero concentration of pollutant (heavier than air) is imposed on the hot wall (C$_c$ = 0) while the cold wall is set at the concentration (C$_h$). We set the Prandtl number at Pr = 0.71, the Planck at 0.02 and the calculation parameters are fixed at Ra=5.10^6, Θ_0=1.5 and Le=1 respectively.

3.1   *Optical thickness effect*

3.1.1   *Cooperating flows*

Firstly, the effects of radiation at different opacities of the medium are examined for the case N = 0$^+$ (see Fig. 3), meaning that the molar mass between gas and the polluting component is low enough that we can neglect the mass buoyancy

forces. In this case, the coupling between the fields of concentration and temperature disappears in the absence of radiation or when the absorption is independent of concentration.
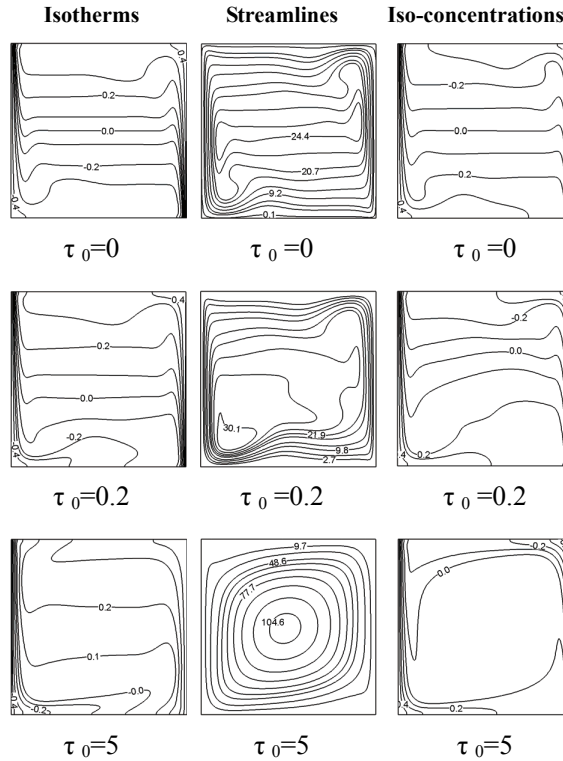
Isotherms	Streamlines	Iso-concentrations

$\tau_0=0$ $\tau_0=0$ $\tau_0=0$

$\tau_0=0.2$ $\tau_0=0.2$ $\tau_0=0.2$

$\tau_0=5$ $\tau_0=5$ $\tau_0=5$

Figure 3: Isotherms, streamlines and iso-concentrations for $N=0^+$ in the case $\tau = 0, 0.2, 5$.

In the absence of radiation effects ($\tau_0 = 0$), the fields of temperature and concentration are identical, and the stratified distribution of temperature in the cavity core explains the resting state of the fluid in this area. Symmetrical movement of the fluid is generated by the strong temperature gradients formed near the active walls. This flow is sensitive to the radiation effects, which is able to change the temperature distribution, especially in the boundary layer near the wall at high concentrations. In doing so, it intensified the gradients along the cold wall. It is to be noted that with increasing optical thickness, temperature profiles become identical. The radiation also causes a general rise in temperature in the isothermal core of the cavity. Some of this heat contribution is evacuated by convection along the cold wall, which explains the increase of the velocity field at this level.

When the environment is sufficiently absorbing, the cold fluid descending towards the bottom wall is heated by absorbing radiant energy emitted by the hot wall. This temperature gradient produces thermal forces that push up the fluid passing over the lower horizontal wall, which explains the low slope of the streamlines near the horizontal walls where τ_0 is greater than 1 (Fig. 3).

More the opacity of the fluid increases, more the concentration field is stratified, due to the intensification of the convective mass transfer in the cavity core (Fig. 3).

3.1.2   Opposing flows

For the opposing flows, the heat and mass forces act in opposite directions. The configuration examined here is the same as that seen previously in the aiding case, with a supplementary permutation in the boundary conditions of concentration. Still remember that this is a square cavity, filled with gas mixtures having the buoyancy ratios N, selected to cover the three convective flow regimes: thermal regime (N<1), intermediate regime (N=1) and mass regime (N>1). The difference between the case $N = 0^-$ and $N = 0^+$ is the permutation of high and low absorption locations by changing the side of the boundary conditions in concentration.

The isotherms, streamlines and iso-concentrations corresponding to ($N=0^-$) are illustrated in Fig. 4. In this configuration, for a transparent gas, the thermal forces are predominant and govern essentially the dynamics of fluid: the flow is multicellular and is circulating in the direction of clockwise, with stratified distribution of temperature and concentration in the cavity core, which explains the resting state of the fluid in this zone. We find that the stagnant cavity core is also set in motion when thermal forces occurred. This behaviour destroys the stratified distribution of concentration field and replaces it with a homogeneous field at the center of the cavity (Fig. 4, gray gas).

The temperature distribution is less changed by the radiation effects (due to the low concentration of radiating species, $N=0^-$). In the upper part, the mixture is cooled by radiation emission, whereas the lower part is heated by the radiation absorption.

3.2   Effects of buoyancy ratio N

3.2.1   Cooperating flows

In the following, we study the influence of buoyancy ratio for different opacities τ_0. Fig. 5 presenting the isotherms, the streamlines and iso-concentrations for various values of N (N= 0, 1 and 15). In the absence of radiation ($\tau_0 = 0$), the main structure of the temperature and concentration does not change substantially according to N variation. When the buoyancy ratio N is larger (greater than 1), the radiation has less effect on the flow dynamics and therefore on the distribution of the pollutant

Isotherms **Streamlines** **Iso-concentrations**

$\tau_0=0$ $\tau_0=0$ $\tau_0=0$

$\tau_0=0.2$ $\tau_0=0.2$ $\tau_0=0.2$
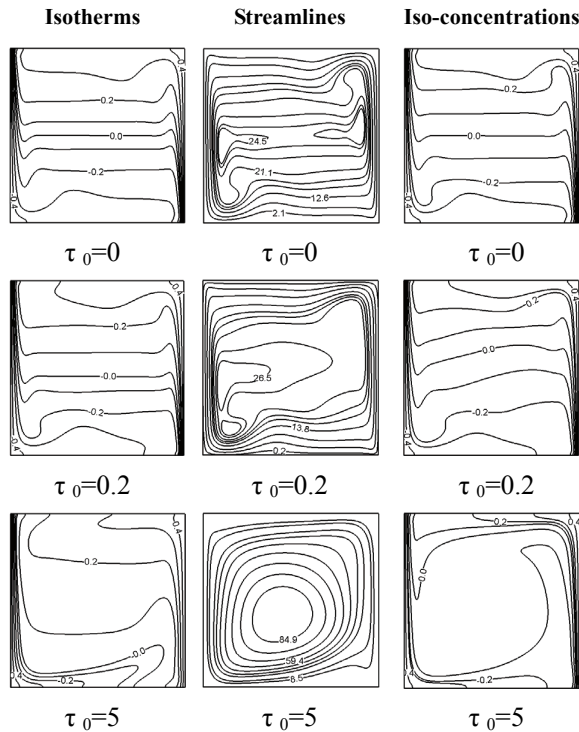
$\tau_0=5$ $\tau_0=5$ $\tau_0=5$

Figure 4: Isotherms, streamlines and iso-concentrations for $N=0^-$

in the cavity. This reflects the fact that when the flow is mainly caused by mass forces, temperature is a passive contaminant and therefore the coupling between the thermal and dynamic fields tends to disappear. Thus, the radiation field will affect neither the velocity nor the concentration field.

In the case, $N=1$, the volumetric radiation significantly alters the dynamic field, including the increase of the fluid flow. But when the mass forces become dominant ($N>1$), the influence of radiation appears at the center of the cavity in term of stratified and inclined isotherms and iso-concentrations (Fig. 5). Thus we find that in this zone, the fluid is at rest, so the resultant force is zero, which explains the inverse slope of the isotherms compared to that of iso-concentrations. Higher values of N promotes the expansion of the central area, but at the same time, causes a decrease of the iso-concentration slope, as shown in Fig. 5.

The distribution of heat transfer by convection along vertical walls, for gas mixture considered, is illustrated in Fig. 6-a.

The average Nusselt number decreases, due to the attenuation of radiative transfer
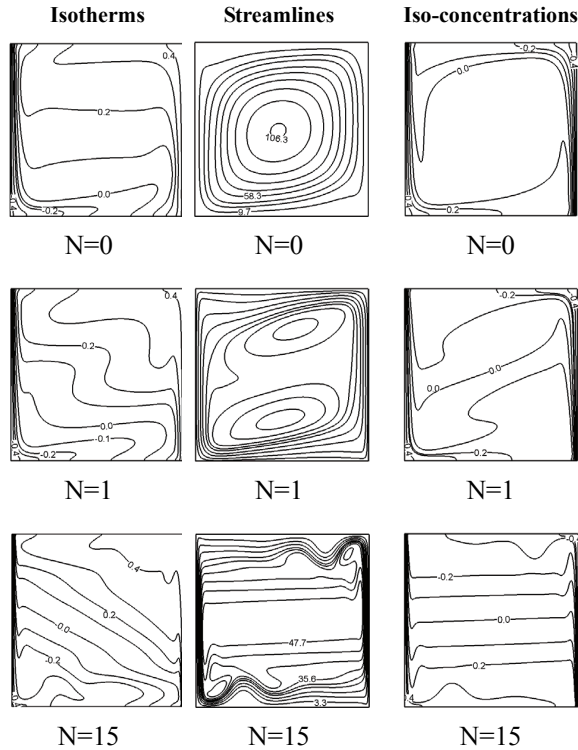
Figure 5: Isotherms, streamlines and iso-concentrations for N=0, 1 and 15 at τ_0=5.

between active walls by the fluid. This attenuation is stronger for higher buoyancy ratio. In other hand, for a given opacity the averaged Nusselt number increases with the buoyancy ratio N. It should be noted that the mass transfer (averaged Sherwood numbers) is slightly affected by the gas radiation (Fig. 6-b).

3.2.2 *Opposing flows*

When the results obtained for $N = 0^-$ (Fig. 4) are compared with those obtained for the case $N = 0^+$ (Fig. 3), we note that for a fixed opacity, the effects of radiation in the first case are weaker than in the second ($N = 0^+$). The increase of the temperature gradient along the cold wall is lower for $N = 0^-$ than it was at $N = 0^+$. In fact, in the latter case, the fluid (concentrated, so absorbent) is heated by radiation but in the case of $N = 0^-$, the fluid is weakly concentrated (and therefore less absorbing in this region), which explains the low horizontal velocity along the lower wall in case $N = 0^-$. Conversely, the gradient along the hot wall is stronger at $N = 0^-$ than at $N = 0^+$. However, the flow is lower at $N = 0^-$ than at $N = 0^+$, as
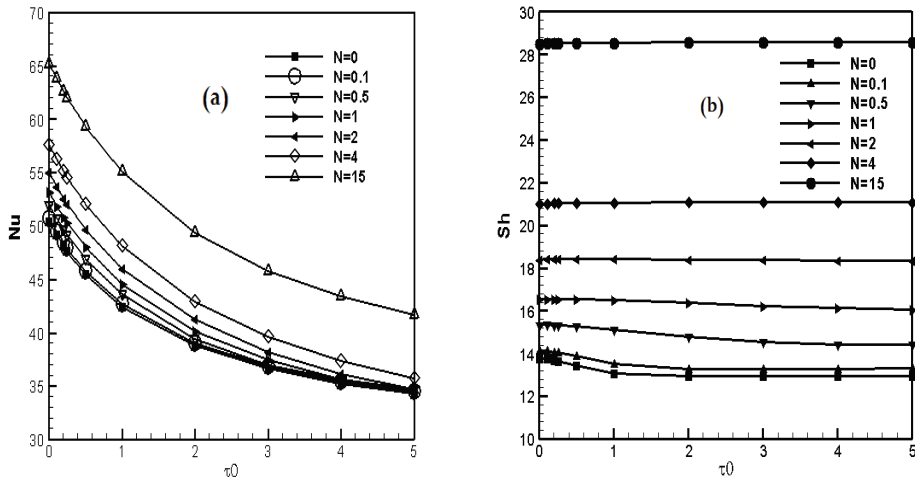
Figure 6: (a) Average Nusselt number, (b) Average Sherwood number, versus τ_0
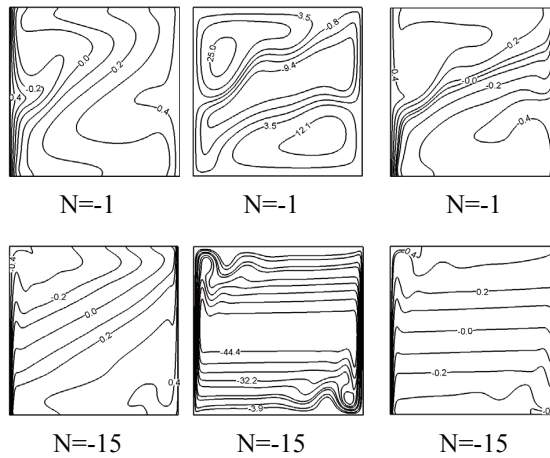
shown in streamlines obtained for both cases.

N=-1	N=-1	N=-1

| N=-15 | N=-15 | N=-15 |

Figure 7: Isotherms, streamlines and iso-concentrations for $\tau_0 = 5$

When the buoyancy ratio N is greater than 1 in absolute value, as illustrated in Fig. 7. For transparent gas, the mass forces dominate the dynamics of the fluid and create a mono-cellular flow in the opposite direction clockwise (transparent gas). In the presence of gas radiation, thermal forces are reinforced in horizontal walls (increased gradients) where the mass forces are dominant. Since these two

types of forces are opposite, their resultant is reduced, causing a slowdown (or even stop) of the horizontal boundary layers (Fig. 7). Vertical boundary layers are also slowed, but only in lower part for the left wall and in higher part for the right wall. This redistribution of velocities in the boundary layer (partial and non-uniform slow) causes the inclination of the streamlines and slight destruction of the centro-symmetry of the dynamic field. While the mass forces are dominant, the monocellular structure of flow field is maintained.

Regarding the concentration field, Fig. 7 shows that the iso-concentrations in center of the cavity are inclined in presence of radiation effects. This behaviour, already observed in a cooperating flow is due to the slowdown of the boundary layers. Indeed, at constant concentration imposed on the walls, an excess of pollutant will appear near the middle of the left wall (at C_h) and a deficit near the middle of the right wall (C_c=0). Negative horizontal gradients of concentration (pollutant diffusion from left to right) arise within the cavity, which gives this tilted structure of concentration field.

Figs. 8-a-b show the variations of averaged Nusselt and Sherwood numbers as a function of the opacity of the medium for different values of N in opposing flow.
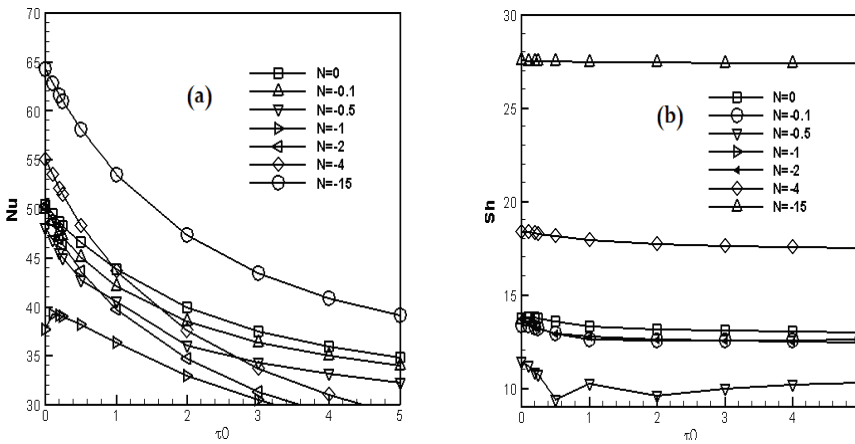

Figure 8: (a) Average Nusselt number, (b) Average Sherwood number, versus τ_0

The behaviour of the averaged total Nusselt numbers (convective and radiative) in the presence of radiation (Fig. 8-a), is less affected than in it absence. Their decline is due to the attenuation of radiative transfer between active walls by the fluid. Logically, this attenuation is stronger when the average concentration of the radiant species increases.

Regarding mass transfer, the local Sherwood numbers in the opposing case (Fig. 8-b) are also more sensitive to radiation than for aiding case. The most important effects are observed when mass and heat buoyancy forces are comparable, corresponding to the intermediate convective regime. The evolution of the average Sherwood number depending on the optical thickness shows that the average mass fluxes at the walls are almost insensitive to radiation in the thermal regime (as in the cooperating flow case). They have increased in the intermediate regime (due to increased flow in the heat cells) and reduced in the mass regime (because of the slowdown of the boundary layers).

3.3 Effects of Rayleigh number

The isotherms and streamlines are shown in Fig. 9 for Rayleigh numbers ranging from 10^3 to 10^7 characterizing the laminar flow regime. Two values of the optical thickness (τ_0=5 and -5) are considered. The Planck number is set equal to 0.02 and for the following calculations, Ra is varied by assuming that the temperature difference ΔT between the hot and the cold walls varies while the mean temperature T_0 is fixed. Thus the reference temperature ratio is simultaneously adjusted by: Θ_0=7.5/(Ra.10^{-6}).

According to the Fig. 9, when the radiation effects are taken into account especially for small values of *Ra*, the isotherms are quasi-verticals and more intensified close to the left cold wall of the cavity. The isotherms deviate from the initial vertical state when Ra reaches 10^7. As can be seen on these figures, while the Rayleigh number increases, the effect of radiation on isotherms and iso-concentrations is restricted to the cavity centre where stratified and inclined profiles of temperature and concentration appear (see Fig. 9). We note that in the core of the cavity, the fluid is stagnant, i.e. the resulting force is null in this region, which explains the opposite slopes of the isotherms and iso-concentrations.

The volumetric radiation causes an acceleration of the fluid in the cavity compared to the case without radiation, but the structure flow is conserved. Generally for the cooperating flows and when the optical thickness τ_0 is fixed, the radiation effect decreases with increasing *N*.

The effect of the Rayleigh number on the isotherms and iso-concentrations in the opposing flows case is the same as the cooperating flow for transparent and opaque fluids with the existence of strong slope of the isotherms, which implies the presence of the high thermal gradients tending to counterbalance the mass forces in the centre of the cavity. However, the inclined streamlines close to the horizontal walls, owing to the radiation, are more apparent. When N is raised, the radiation influence on the iso-concentrations and streamlines becomes negligible (Fig. 9) because, in this case, the temperature plays just the role of a passive contaminant.
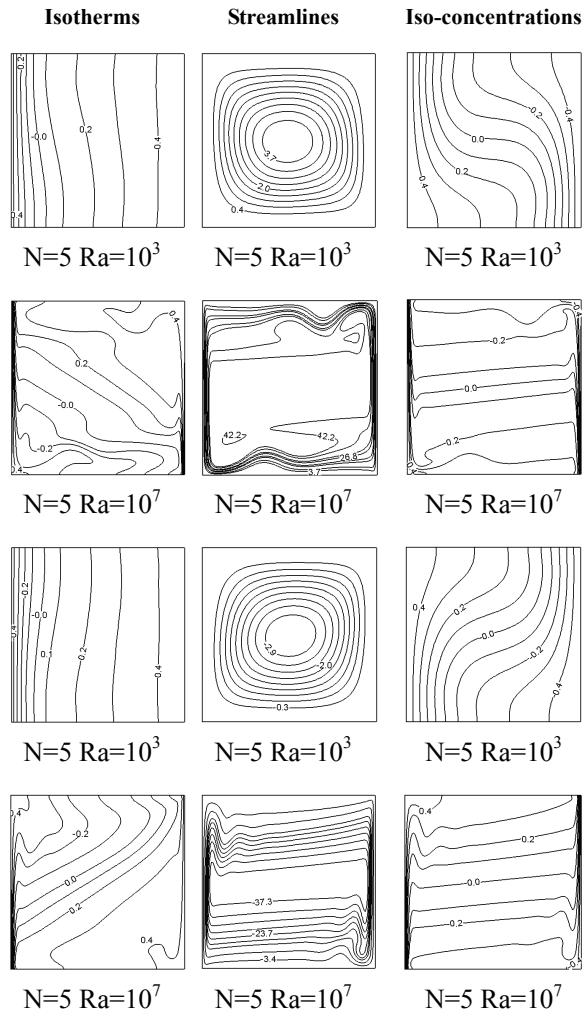
Isotherms	**Streamlines**	**Iso-concentrations**

Figure 9: Isotherms, streamlines and iso-concentrations for N=5, τ_0=5 and Ra=10^3-10^7

Fig. 10-a shows in the cooperating flows that the averaged Nusselt number increase as function of the increasing of Rayleigh number and decrease versus the increase of the optical thickness. The heat transfer is augmented when the buoyancy ratio N rises. The mass transfer follows the same behaviour versus the Rayleigh variation but it is insensitive to the opacity of the medium (Fig. 10-b).

In opposing flow case (Fig. 11-a-b), the heat and mass transfer increase as the buoyancy ratio N increase in absolute value and decrease as function of the opacity
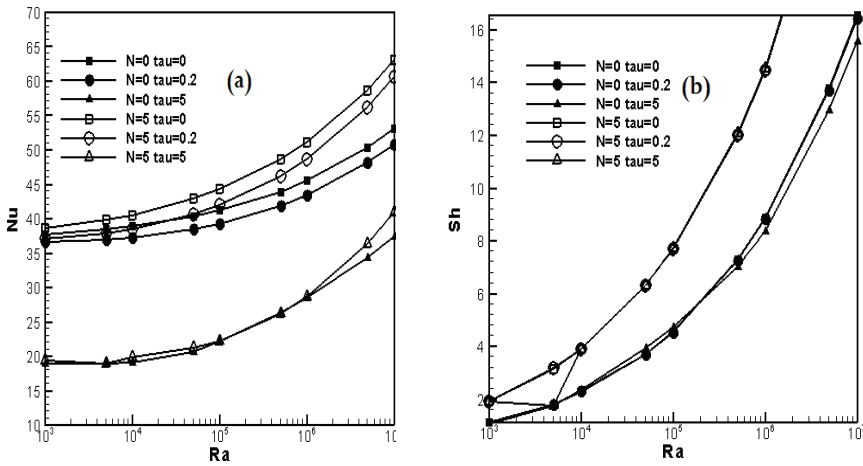
Figure 10: (a) Average Nusselt number, (b) Average Sherwood number, versus Ra for N= 0, 5

increase. It's obvious that the heat and mass transfer has slightly the same magnitude as in the cooperation flows with the same buoyancy ratio N.
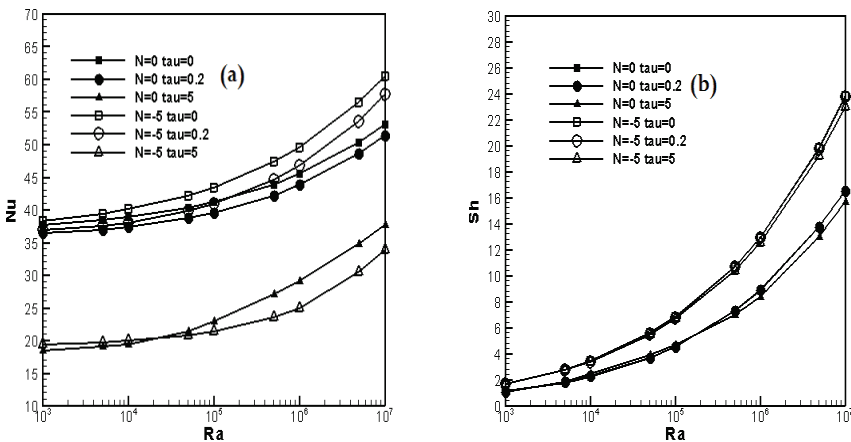

Figure 11: (a) Average Nusselt number, (b) Average Sherwood number, versus Ra for N= 0, -5

It is found that, the increase of Rayleigh number always decreases the influence of radiation in cooperating flow. However, in the opposing flow, it may, also in a

certain interval, increase the effects of radiation. The width of this interval depends on both the opacity of the medium and the buoyancy ratio. More τ_0 is large (we studied up to 5), over the interval widens. Regarding mass transfer, generally, the influence of Rayleigh number is practically the same in the presence or in absence of radiation (the maximum difference is about 5%). Nevertheless, in opposing flows where the thermal and mass forces are comparable ($1 \leq N \leq 2$), we see a difference due to radiative effects.

3.4 Effects of the Lewis number

The working fluid considered in this study as a binary mixture of gases, this implies that the Lewis number can hardly be outside the interval [0.1, 10], so this area of variation is retained in this study.

For thicker media (Fig. 12) when Le<1, the strong slope and the distortion of isotherms lines signify the existence of a high gradients of temperature in the core cavity which tends to counteract the mass buoyancy forces, but for Le>1 the isotherms stratification is found. There is bicellular configuration of streamlines at Le<1 and monocellular one otherwise. The concentration distribution is less affected when Le<1 except the inclination of iso-concentration lines noted in the case Le=1, in other hand a low mass diffusivity is observed at the center of cavity for a high Lewis numbers.

The analysis of Fig. 13(a) shows that the averaged Nusselt number decreases as function of Lewis number for fixed opacity. For given Lewis number, the averaged Nusselt number decrease when the optical thickness increase. Whereas, the Sherwood number increases with increasing Lewis number. It seems from the Fig. 13 that the optical thickness variation doesn't affect the mass transfer (see Fig. 13(b)).

In the opposing flow case, the isotherms, iso-concentrations and streamlines are examined for the case when the thermal and mass forces are equivalents.

The analysis of Fig. 14, shows that the isotherms are denser at boundary layers and the resting state of the core is broken (Le<1). For Le=1 a strong slop is observed in isotherms, but the high temperature gradients in active walls homogenize the temperature structure in the core for Le>1. A multicellular structure is noted for the case Le<1 and monocellular flow is done for Le>1. The structure with three cells characterizes the Le=1 case. The stratification of iso-concentration is slightly destroyed at Le<1 and the iso-concentration lines are inclined for Le=1. These lines move out the core of the cavity when Le greater than 1.

From the Fig. 15(a), we note that the heat transfer decrease as function the Lewis number increase for fixed opacity and also decrease when the optical thickness increase at given Lewis number. Regarding the mass transfer, the averaged Sherwood
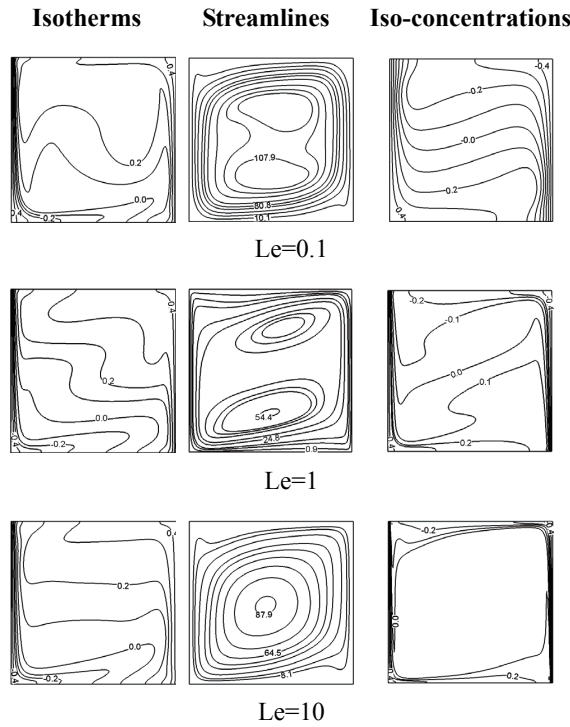
Isotherms   **Streamlines**   **Iso-concentrations**

Le=0.1

Le=1

Le=10

Figure 12: Isotherms, streamlines and iso-concentrations for τ_0=5 and N=1

number increase with Lewis number and it is not much sensitive to the opacity variation (see Fig. 15(b)).

According to the previous analysis, when the Lewis number increased in the absence of radiation, the intervention area of mass forces is reduced and the flow velocity decreases. This causes a sharp drop in heat transfer by convection at the walls (remember that the flow velocity near the wall was directly related to heat transfer by conduction at this level). Contrary, in the presence of radiation, the temperature gradient along the hot wall becomes weak, which favours the dominance of mass forces and reduces the drop in velocity due to the increase of Lewis number.

4   Conclusion

In conclusion, the radiation accelerates the boundary layer but maintains the cavity core stagnant. In other hand the temperature and concentration fields are also altered, especially by creating a structure with tilted iso-values. The gas radiation
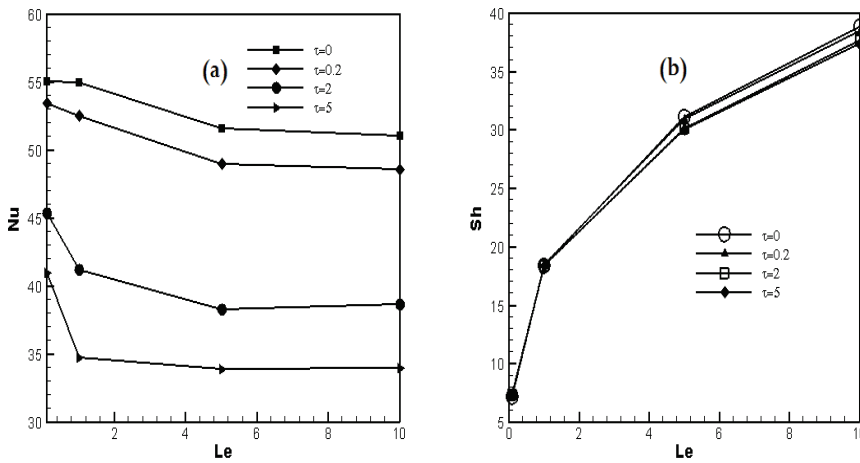
Figure 13: (a) Average Nusselt numbers, (b) Average Sherwood numbers, versus Le for N=2
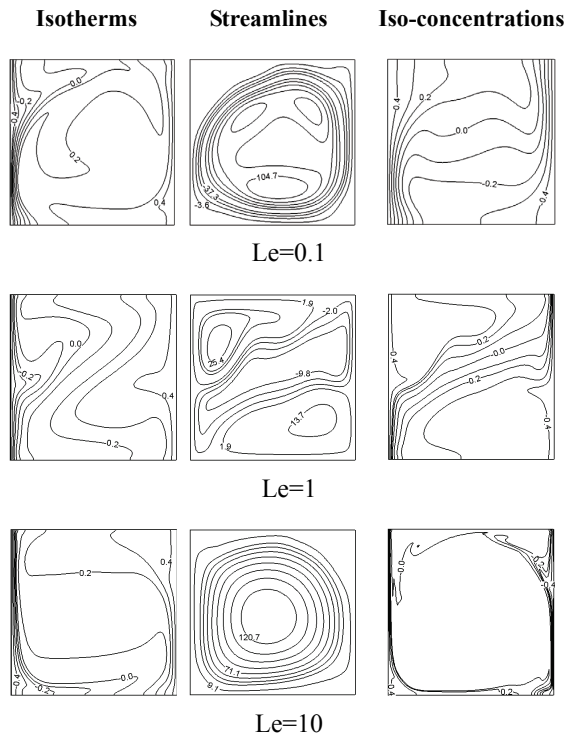
Isotherms **Streamlines** **Iso-concentrations**

Le=0.1

Le=1

Le=10

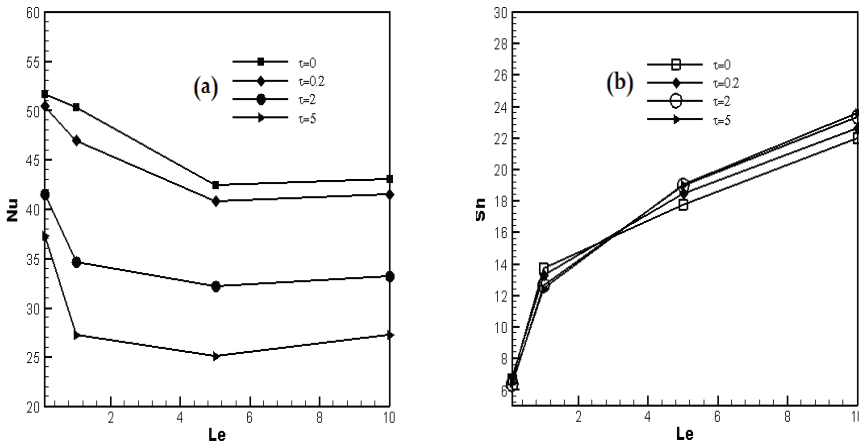Figure 14: Isotherms, streamlines and iso-concentrations for $\tau_0 = 5$ and N=1

Figure 15: (a) Average Nusselt number, (b) Average Sherwood number, versus *Le* for N=2

reduces the heat transfer (convective and total), but has practically no influence on mass transfer. The increase of the optical thickness causes an increase in temperature and thereafter modifying the fluid flow. In general, the flow is lower in opposing case than in the cooperating case. In other side the effect of radiation, longer changes the flow dynamics in the aiding case that in opposing case, especially when the buoyancy forces ratio N is increased.

We can deduce for cooperating flows that in the presence of radiation, the temperature gradient along the hot wall becomes weak, which favours the dominance of mass forces and reduces the drop in velocity due to the increase of Lewis number. The opposing flows with a smaller Lewis number are characterized by stratified structure having a conduction mode dominance and oscillatory structure flow otherwise. Generally, the heat transfer is less important than it is for transparent media, but the mass transfer is not much affected when the optical thickness is varied.

References

Balaji, C.; Vankateshan, S.P. (1994): Correlation for free convection and surface radiation in a square cavity, *Int. J. Heat and Fluid Flow*, vol. 15, pp. 249-252.

Bhatnagar, P.; Gross, E.; Krook, M. (1954): A model for collision process in gases. I. Small amplitude process in charged and neutral one-component systems, *Physical Review*, vol. 94, pp. 511-525.

Borjini, M. N.; Ben Aissia, H.; Halouani, K.; Zeghmati, B. (2006): Effect of

optical properties on oscillatory hydromagnetic double-diffusive convection within semitransparent fluid, *Int. J. Heat Mass Transfer*, vol. 49, pp. 3984–3996.

Chandrasekhar, S. (1950): *Radiative transfer*, Clarendon Press.

Choukairy, K.; Bennacer, R.; Beji, H. ; El Ganaoui, M. ; Jaballah, S. (2006):Transient behaviours inside a vertical cylindrical enclosure heated from the side walls. *Num. Heat Transfer,* part A, vol. 50, pp. 1-13.

D'Humières, D. (1992): Generalized lattice Boltzmann equations Rarefied Gas Dynamics: Theory and Simulations (Progress in Astronautics and Aeronautics). *ed. B D Shizgal and D P Weaver (Washington, DC)*, vol. 8, pp. 450.

Fiveland, W.A (1984): Discrete-ordinates solution of the radiative transport equation for rectangular enclosures, *J. Heat Transfer*, vol. 106, pp. 699-706.

Ganesan, P.; Loganathan, P. (2002): Radiation and mass transfer effects on flow incompressible viscous fluid past a moving vertical cylinder, *Int. J. Heat Mass Transfer*, vol. 45, pp. 4281-4288.

Ghorayeb, K.; Khallouf, H.; Mojtabi, A. (1999): Onset of oscillatory flows in double diffusive convection, *Int. J. of Heat Mass Transfer*, vol. 42, pp. 629-643.

Gobin, D.; Goyeau, B.; Neculae, A. (2005) : Convective heat and solute transfer in partially porous cavities, *Int. J. Heat Mass Transfer*, vol. 48, pp. 1898-1908.

Hu, C.Y.; El-Wakil, M.M. (1974): Simultaneous heat and mass transfer in a rectangular cavity. *Int. Heat Transfer Conf.*, Tokyo, Japan, vol. 5, pp. 24.

Kassemi, M.; Naraghi, M.H.N. (1993): Analysis of radiation-natural convection interactions in 1-G and low-G environments using the discrete exchange factor method. *Int. J. of Heat and Mass Transfer*, vol. 36, pp. 4141-4149.

Lallemand, P.; Luo, L S. (2000): Theory of the lattice Boltzmann method: dispersion, dissipation, isotropy, Galilean invariance and stability, *Phys. Rev.,* vol. E 61, pp. 6546-6562.

Lallemand, P.; Luo, L.S. (2003): Lattice Boltzmann method for moving boundaries, *J. Comput. Phys.*, vol. 184, pp. 406-421.

Lauriat, G. (1982): Combined radiation-convection in gray fluids enclosed in vertical cavities, *J. Heat Transfer*, vol. 104, pp. 609-615.

Meftah, S. (2010): *Modeling of Natural double diffusion convection in mixture gases absorbing and emitting radiation*, PhD thesis, University M'hamed Bougara–Boumerdes Algeria.

Mezrhab, A.; Lemonnier, D.; Meftah, S. ; Benbrik, A. (2008): Numerical study of double diffusion convection coupled to radiation in a square cavity filled with a participating grey gas, *J. Phys. D: Appl. Phys*, vol. 41, pp. 5501-5517.

Mezrhab, A.; Moussaoui, M.A.; Naji, H. (2008): Lattice Boltzmann simulation of surface radiation and natural convection in a square cavity with an inner cylinder, *J. Phys. D: Applied Physics*, vol. 41, pp. 551-557.

Mohamad, A.A.; Bennacer, R.; El-Ganaoui, M. (2010): Double dispersion, natural convection in an open end cavity simulation via Lattice Boltzmann Method. *Int. Journal of Thermal Sciences,* vol. 49, no.10, pp. 1944-1953.

Moufekkir, F.; Moussaoui, M.A.; Mezrhab, A.; Lemonnier, D.; Naji, H. (2012): MRT-lattice Boltzmann computations of natural convection and volumetric radiation in a tilted square enclosure. *Int. Journal of Thermal Sciences*, vol. 54, pp. 125-141.

Moussaoui, M.A.; Jami, M.; Mezrhab, A.; Naji,H. (2010): MRT-Lattice Boltzmann simulation of forced convection in a plane channel with an inclined square cylinder, *I. J. of Thermal Sciences*, vol. 49, pp. 131-142.

Rafieivand, M. (1999) : *Etude numérique de la convection de double diffusion en présence de rayonnement en cavité rectangulaire*, Thèse de Doctorat, Université de Poitiers, Poitiers, France.

Ramachandra Prasad, V.; Bhaskar Reddy, N. ; Muthucumaraswamy, R. (2007): Radiation and mass transfer effects on two-dimensional flow past an impulsively started infinite vertical plate, *Int. J. Therm. Sci*, vol. 46, pp. 1251-1258.

Semma, E.; El Ganaoui, M.; Mohamad., R. A.A. (2008): Investigation of flows in solidification by using the lattice Boltzmann method, *Int. Journal of Thermal Sciences,* vol. 47, pp. 201-208.

Tan, Z.; Howell, J R. (1991): Combined radiation and natural convection in a square enclosure with participating medium, *Int. J. Heat Mass Transfer*, vol. 34, pp. 785-793.

Trevisan, O.V.; Bejan, A. (1987): Combined heat and mass transfer by natural convection in a vertical enclosure. *Int. J. Heat Transfer*, vol. 109, pp. 104-112.

Truelove, J.S. (1988): Three-dimensional radiation in absorbing-emitting-scattering in using the discrete-ordinates approximation, *JQSRT*, vol. 39, pp. 27-31.

Viskanta, R.; Bergman, T.L.; Incopera, F.P. (1985): *Double-diffusive natural convection. In Natural Convection, Fundamentals and Applications.* Hemisphere, Washington DC, pp. 1075.

Yucel, A.; Acharya, S.; Williams, M.L. (1989): Natural convection and radiation in a square enclosure, *Numer. Heat Transfer*, vol. A 15, pp. 261-278.